HHS Public Access

Author manuscript

J Bone Miner Res. Author manuscript; available in PMC 2016 April 01.

Published in final edited form as:

J Bone Miner Res. 2015 April ; 30(4): 723–732. doi:10.1002/jbmr.2378.

A single nucleotide polymorphism in osteonectin 3' untranslated region regulates bone volume and is targeted by miR-433

Neha S. Dole, M.S.[1], **Kristina Kapinas, Ph.D.**[1], **Catherine B. Kessler, B.S.**[1], **Siu-Pok Yee, Ph.D.**[2], **Douglas J. Adams, Ph.D.**[3], **Renata C. Pereira, Ph.D.**[4], and **Anne M. Delany, Ph.D.**[1]

[1]Center for Molecular Medicine, University of Connecticut Health Center, Farmington, CT, U.S.A.

[2]Gene Targeting and Transgenic Facility, University of Connecticut Health Center, Farmington, CT, U.S.A.

[3]Department of Orthopaedic Surgery, University of Connecticut Health Center, Farmington, CT, U.S.A.

[4] Mattel Children's Hospital, University of California, Los Angeles, CA, U.S.A.

Abstract

Osteonectin/SPARC is one of the most abundant non-collagenous extracellular matrix proteins in bone, regulating collagen fiber assembly and promoting osteoblast differentiation. Osteonectin-null and –haploinsufficient mice have low turnover osteopenia, indicating that osteonectin contributes to normal bone formation. In male idiopathic osteoporosis patients, osteonectin 3' UTR single nucleotide polymorphism (SNP) haplotypes that differed only at SNP1599 (rs1054204) were previously associated with bone mass. Haplotype A (containing SNP1599G) was more frequent in severely affected patients, whereas haplotype B (containing SNP1599C) was more frequent in less affected patients and healthy controls. We hypothesized that SNP1599 contributes to variability in bone mass by modulating osteonectin levels. Osteonectin 3'UTR reporter constructs demonstrated that haplotype A has a repressive effect on gene expression compared to B. We found that SNP1599G contributed to a miR-433 binding site and miR-433 inhibitor relieved repression of the haplotype A, but not B, 3' UTR reporter construct.

We tested our hypothesis in vivo, using a knock-in approach to replace the mouse osteonectin 3' UTR with human haplotype A or B 3' UTR. Compared to haplotype A mice, bone osteonectin levels were higher in haplotype B mice. B mice displayed higher bone formation rate and gained more trabecular bone with age. When parathyroid hormone was administered intermittently, haplotype B mice gained more cortical bone area than A mice. Cultured marrow stromal cells from B mice deposited more mineralized matrix and had higher osteocalcin mRNA compared with A mice, demonstrating a cell-autonomous effect on differentiation. Altogether, SNP1599

To whom correspondence should be addressed: Anne Delany, Center for Molecular Medicine, University of Connecticut Health Center, 263 Farmington Ave, Farmington, CT, 06030, USA, Tel: (860)679-8730; Fax: (860) 679-1258, adelany@uchc.edu.

Author contributions: NSD, KK, SPY and AMD designed the research. NSD, KK, CBK, DJA, RCR, and AMD performed the research and analyzed the data. NSD and AMD wrote the manuscript and take responsibility for the data analysis. All authors approved of manuscript submission.

Disclosure page.

All authors state that they have no conflicts of interest.

differentially regulates osteonectin expression and contributes to variability in bone mass, by a mechanism that may involve differential targeting by miR-433. This work validates the findings of the previous candidate gene study, and it assigns a physiological function to a common osteonectin allele, providing support for its role in the complex trait of skeletal phenotype.

Keywords

Osteoporosis; Molecular pathways – remodeling; Genetic animal models; Non-collagenous proteins; Human association studies

Introduction

Osteoporosis is a prevalent disorder characterized by low bone mineral density (BMD), deterioration of bone microarchitecture and increased incidence of fracture;[1] and genetic factors account for 60-80% of total variability in BMD.[2] Understanding the genetic determinants underlying bone mass may improve prognosis and provide novel targets for therapeutic intervention. In this regard, genome wide association studies (GWAS) and candidate gene studies have associated allelic variants of genes such as estrogen receptor (ER)-α, transforming growth factor (TGF)-β, osteoprotegerin, and type I collagen A1 with bone mass.[3-6] However, only a few studies have demonstrated a mechanism whereby a polymorphism could contribute to bone mass phenotype.

Indeed, a previous GWAS study in premenopausal women linked variations in BMD to genomic regions including 5q33-35.[7] Although candidate genes in the 5q33-35 interval were not identified, this region contains the gene for osteonectin/*Sparc* (secreted protein acidic and rich in cysteine), one of the most abundant non-collagenous extracellular matrix proteins in bone. In osteoblasts, osteonectin promotes commitment, differentiation, and survival. Osteonectin also suppresses adipogenic differentiation of mesenchymal precursor cells. In vivo, osteonectin-null and –haploinsufficient mice develop low turnover osteopenia, characterized by reduced osteoblast and osteoclast number and surface, and low bone formation rate.[8-12] Moreover, osteonectin-null mice accumulate less bone in response to intermittent administration of parathyroid hormone (PTH), the best bone-anabolic treatment clinically available at this time.[12]

Based on these findings, we had previously performed a candidate gene study, to determine whether 3 single nucleotide polymorphisms (SNPs) in the 3’ untranslated region (UTR) of osteonectin (Figure 1A) were associated with bone mass in a cohort of men with low turnover idiopathic osteoporosis, a disorder primarily attributed to genetic determinants.[13] Briefly, this cohort consisted of middle aged Caucasian men with a BMD T score of less than −2.0 at the lumbar spine, who lacked known secondary causes for osteoporosis. The control subjects were age and body mass index matched to the patients, and had BMD T scores of more than 1.0 at the lumbar spine. As a group, the idiopathic osteoporosis patients had mean serum PTH and IGF1 levels in the low normal range. Their indices of bone formation were significantly reduced, although eroded surface was not different between patients and their matched controls. [14, 15] In the osteoporotic cohort, prevalence of fragility fracture was 23%. [13]

In this cohort, one of the two most common osteonectin 3' UTR haplotypes that we identified, haplotype A, was found at a higher frequency in the most severely affected osteoporotic patients, whereas the second most common haplotype, B, was found at a higher frequency in the healthy controls. In addition, haplotype B was associated with higher BMD in the patient population.[13] Osteonectin 3' UTR haplotype A contained the SNPs at cDNA bases 1046C_1599G_1970T, whereas haplotype B consisted of SNPs 1046C_1599C_1970T (Figure 1A). Since these BMD-associated haplotypes differed only at cDNA base 1599, we hypothesized that SNP 1599G/C (rs1054204) may impact osteonectin expression, and affect bone mass.

The 3' UTR represents a powerful regulatory region, with the potential to modulate mRNA stability, translation and localization.[16] Polymorphisms in the 3' UTR have the potential to alter the secondary structure of the mRNA, as well as its interaction with trans-acting factors, such as microRNAs (miRNAs, miRs). miRNAs are small, endogenous non-coding RNAs that, for the most part, decrease the stability and/or translation of protein-encoding mRNAs.

Recent studies have associated mutations or SNPs in miRNA binding with skeletal disorders. For example, a SNP in the 3' UTR of *Fgf2* (fibroblast growth factor 2), that abrogates miR-146a and -146b binding sites, was linked to low BMD in osteoporotic patients.[17] Another study attributed a mutation in the binding site for miR-433 in the 3' UTR of *Hdac6* (histone deacetylase 6) to the pathogenesis of X-linked chondrodysplasia.[18]

In this study we show that human osteonectin SNP1599 differentially regulates gene expression and contributes to a miR-433 binding site. Specifically, 1599G, found in haplotype A, has a repressive effect on gene expression and osteoblastic differentiation compared to 1599C, which is found in haplotype B. Moreover, using novel knock-in mouse models, we demonstrate that compared to mice carrying human osteonectin haplotype A 3' UTR (SNP 1599G), mice with the haplotype B 3' UTR knock-in (SNP 1599C) have higher levels of osteonectin in bone, higher bone formation rate, increased trabecular bone volume with age, and a greater increase in cortical bone volume in response to the bone-anabolic PTH treatment. These data substantiate the relationship between osteonectin 3' UTR SNP 1599 and skeletal phenotype, validate our initial observations in the cohort of idiopathic osteoporosis patients, and suggest that SNP 1599 affects bone mass by modulating osteonectin expression.

Materials and Methods

Generation of osteonectin 3' UTR haplotype constructs

Human osteonectin 3' UTR (cDNA bases 1018-2123) representing haplotypes A and B found in idiopathic osteoporosis patients were PCR amplified from genomic DNA and cloned downstream of the Luciferase gene in pMIR-REPORT vector (Life Technologies). Details of cloning are described in *Supporting Information (SI)* text.

Cell culture, transfection and luciferase activity

Human fetal osteoblastic 1.19 cell line (hFOB1.19) was purchased from American Type Culture Collection (ATCC number CRL-11372) and were grown at 33.5° C and differentiated into osteoblast cultures at 39.5° C in the presence of differentiation cocktail: 100 μg/mL ascorbic acid, 10^{-8} M menadione (Vitamin K), 5 mM β-glycerolphosphate (β-GP), and 10^{-7} M 1-25$(OH)_2$-Vitamin D_3 (all from Sigma, St Louis, MO).[19, 20] Bone marrow stromal cells (BMSCs) harvested from long bones of mice were differentiated in presence of 5 mM β-Glycerolphosphate and 50 μg/mL ascorbic acid. [8, 11]

Haplotype A and B 3' UTR luciferase constructs were transfected into hFOB1.19 cells using Fugene6 (Roche, Indianapolis, IN). For co-transfection of miRNA inhibitors or mimics and luciferase constructs into hFOB1.19 cells, X-tremeGENE reagent (X-tremeGENE; Roche) was used. Details of cell culture and transfection are described in *SI* text.

Generation of osteonectin knock-in mice

A knock-in strategy was used to replace the mouse osteonectin 3' UTR with human haplotype A or haplotype B 3' UTR. These mouse models were generated at the Gene Targeting and Transgenic Facility at UCHC. Osteonectin haplotype A ($ON^{+/A}$) and haplotype B ($ON^{+/B}$) mice were generated using 129 embryonic stem cells and were back crossed into C57BL/6J. Mice heterozygous for A and B alleles ($ON^{A/B}$) were bred to create homozygous A and B mice ($ON^{A/A}$ and $ON^{B/B}$).

Quantitative RT-PCR analysis

RNA was extracted using the miRNeasy mini kit (Qiagen, Valencia, CA). miR-433 levels were determined using the TaqMan MicroRNA assay (Life Technologies, Grand Island, NY) and normalized to RNU48 for human tissue or sno202 RNA for mouse tissue. Osteonectin, alkaline phosphatase, osteocalcin, and bone sialoprotein (Ibsp) mRNA levels were determined using MMLV-Reserve Transcriptase (Invitrogen) and iQ SYBR Green Supermix (BioRad) and normalized to 18sRNA. Primer sequences and details of quantitative RT-PCR are described in *SI* text.

Western blot analysis

Equal amounts of long bone extract were subjected to Western blot analysis for osteonectin and β-actin. Rabbit anti-bovine osteonectin primary antibody (BON-1; gift of L. Fisher, NIDCR, NIH) (1:4000), rabbit anti-β-actin primary antibody (Abcam, 1:1000), and goat anti-rabbit-horseradish peroxidase conjugated secondary antibody (1:20,000) were used. Experimental details of this are described in *SI* text.

Osteoblast differentiation, mineralization and proliferation analysis

BMSCs harvested from long bones were cultured in osteoblast differentiation medium. Cultures were stained with either 1% Alizarin red S pH 6.45 (Sigma) or 0.05% Crystal violet stain (Fisher Scientific). Alizarin red stain was quantified at absorbance 405 nm, while Crystal Violet stain was measured at 570 nm, as described in *SI* text. Cell proliferation was

assessed using MTS CellTiter 96® AQueous One Solution cell proliferation assay kit (Promega, Madison, USA), according to the manufacturer's instructions.

Morphological analysis

To study bone-anabolic response, 10-week old male mice were injected subcutaneously with 40 μg/kg/day rhPTH (1–34) (PTH) (Bachem, Torrance, CA) or vehicle alone (2% heat inactivated mouse serum in acidified saline), 5 days per week for 4 weeks.[12] Details of μCT imaging and histomorphometry of femurs are described in *SI* text. All procedures were approved by the Institutional Animal Care and Use Committee at UCHC.

Statistics

All the quantitative data are expressed as a mean ± SEM. Statistical significance was determined by one-way ANOVA with Bonferroni post-hoc test or Student's t-test. Allele frequencies were evaluated using the Freeman-Halton extension of Fisher's exact test.

Results

SNP 1599 modulates osteonectin 3' UTR function and represses haplotype A 3' UTR

To determine the role of SNP 1599 in regulating the osteonectin 3' UTR, we cloned the 1 kb osteonectin 3' UTR, representing human haplotype A or B, into a Luciferase reporter construct. In these reporter constructs, the cloned sequence functioned as 3' UTR for the Luciferase gene, the transcription of which was constitutively driven by a strong promoter. The constructs were transiently transfected into hFOB1.19 cells, a conditionally immortalized human osteoblastic cell line. We found that the haplotype A 3' UTR construct had lower luciferase activity compared to haplotype B, suggesting that haplotype A, which was found at a higher frequency in the most severely affected osteoporosis patients, had a more repressive effect on gene expression (Figure 1B). These data indicate that SNP 1599 contributed to differences in osteonectin 3' UTR function.

SNP 1599 introduces a novel miR-433 binding site in haplotype A 3' UTR

To determine whether miRNAs may mediate the differential regulation of osteonectin by SNP 1599G/C, we used RNAhybrid (http://bibiserv.techfak.uni-bielefeld.de/bibi/Tools.html) and miRbase v15.0 to assemble a panel of candidate miRNAs with the potential to interact with the region containing SNP 1599. [21] The list of candidate miRNAs was further refined, based on whether or not SNP 1599 would facilitate or disrupt the interaction of the miRNA with the osteonectin 3' UTR. We observed the potential for differential interaction of miR-433-3p, miR-493-5p and miR-374a-3p in presence of 1599G (haplotype A), compared with 1599C (haplotype B) (Table 1). Moreover, these miRNAs are expressed in hFOB1.19 cells.

To test the hypothesis that the candidate miRNAs may differentially target haplotypes A and B in vitro, hFOB1.19 cells were transiently co-transfected with either haplotype A or B 3' UTR reporter constructs and inhibitor for miR-433-3p, miR-493-5p or miR-374a-3p. In the presence of miR-433 inhibitor, luciferase activity of the haplotype A construct was significantly increased compared to the non-targeting control, whereas activity of the

haplotype B construct was not affected. In contrast, inhibitor for miR-374a-3p or miR-493-5p did not significantly increase luciferase expression from either haplotype A or B constructs (Figure 2A). miR-433 targeting of haplotype A 3' UTR was also evaluated in hFOB1.19 cells using miR-433 mimic and a scramble mimic control. In the presence of miR-433 mimic, haplotype A 3' UTR luciferase activity was inhibited compared to the control, whereas haplotype B 3' UTR activity was not significantly affected (Figure 2B).

These results suggest that SNP 1599 introduces a novel miR-433 binding site in haplotype A 3' UTR, which may contribute to differential regulation of osteonectin. However, our data do not preclude the possibility that other miRNAs or trans-acting factors could also demonstrate differential regulation of the haplotype A and B 3' UTRs.

miR-433 expression decreases during osteoblastic differentiation

Since miR-433 could differentially regulate the human osteonectin 3' UTR, we determined whether the expression of this miRNA was altered during osteoblastic differentiation, using hFOB1.19 cells as a model.[19, 20] Osteoblastic differentiation was induced using a vitamin D-containing cocktail, and after 3 or 6 days, mRNAs for the early osteoblastic marker alkaline phosphatase (ALP), and the mature osteoblast marker, osteocalcin (OC), were dramatically increased. In contrast, expression of miR-433 decreased during differentiation, such that miR-433 levels were lowest when osteoblastic differentiation markers were highest (Figure 2C). A similar phenomenon was reported by others when miR-433 levels were evaluated in a BMP2-treated murine pre-osteoblast cell line.[22]

To determine the role of miR-433 in human osteoblastic differentiation, hFOB1.19 cells were transfected with either a miR-433 inhibitor or a scramble control inhibitor and subjected to osteoblastic differentiation for 3 days. Here, miR-433 inhibitor increased mRNA for the osteoblast markers ALP and OC, compared to the scramble control, confirming that miR-433 is a negative regulator of osteoblast maturation in vitro (Figure 2D).

SNP 1599 affects osteonectin expression in vivo

Many mature miRNAs display sequence conservation across species, and the sequence of mature miR-433 is identical between mouse and human (miRBase). Whereas selected regions of the mouse and human osteonectin 3' UTR are highly conserved, such as the miR-29 binding sites in the proximal portion of the UTR,[23] mouse and human osteonectin are not well conserved in the region containing human SNP1599 (UCSD Genome Browser). Therefore, to examine the impact of SNP 1599 on osteonectin expression in bone in vivo, we used a knock-in strategy to replace the mouse osteonectin 3' UTR with the 1 kb human osteonectin 3' UTR, representing either haplotype A ($ON^{A/A}$) or haplotype B ($ON^{B/B}$) (Figure S1). In relation to other mouse strains, C57Bl/6 mice have a low bone mass phenotype.[24,25] We chose to examine the function of the human osteonectin 3' UTR haplotypes in the C57Bl/6 genetic background because our candidate gene study revealed an association between osteonectin haplotype and bone mass only in the idiopathic osteoporosis patient group. We reasoned that the effect of the osteonectin 3' UTR haplotype might be most apparent in a low bone mass background, where other gene variants may not be

sufficient to rescue a low bone mass phenotype. Moreover, we chose to limit our present analysis to males, to further mimic our previous study in male idiopathic osteoporosis patients.

Osteonectin transcript and protein levels in femur of homozygous haplotype A and B ($ON^{A/A}$ and $ON^{B/B}$) male mice were examined. Western blot analysis of protein extracts demonstrated 2-3 fold lower osteonectin levels in $ON^{A/A}$ femur in comparison to $ON^{B/B}$, indicating that SNP 1599 contributed to differential osteonectin accumulation in bone in vivo (Figure 3B). At the same time, qRT-PCR revealed a ~2 fold increase in osteonectin mRNA in femur of $ON^{A/A}$ mice compared with $ON^{B/B}$ (Figure 3A), while miR-433 levels were similar (Figure S2). This apparent discrepancy may be related to the fact that the protein data represent the accumulation of osteonectin in bone tissue, whereas the RNA data represent a window of gene expression at 6-8 weeks of age.

SNP 1599 affects changes in bone mass with age

Using μCT, we analyzed the skeletal phenotype of male $ON^{A/A}$ and $ON^{B/B}$ mice at 10 and 20 weeks of age. The femurs of 10-week old mice $ON^{A/A}$ and $ON^{B/B}$ displayed similar trabecular and cortical bone parameters (Table 2). At 20 weeks of age, trabecular bone volume and trabecular thickness were significantly higher in $ON^{B/B}$ mice compared with $ON^{A/A}$ (Table 2). When the percentage change in trabecular bone parameters between 10 and 20 weeks was examined, the differences between the two genotypes became more apparent (Figure 3C). For example, between 10 and 20 weeks of age, $ON^{B/B}$ mice realized a 20-25% gain in trabecular bone volume fraction (BVF), while $ON^{A/A}$ mice did not. Trabecular number (Tb.N) decreased with age in both the genotypes, and the decrease was significantly less in $ON^{B/B}$ mice. Trabecular spacing (Tb.Sp.) increased between 10 and 20 weeks of age in $ON^{A/A}$ mice, but not in $ON^{B/B}$ animals (Figure 3C). In contrast, cortical bone area (Ct.Ar.) increased from 10 to 20 weeks of age in both genotypes, to a similar extent (Figure 3D). This was not unexpected, as the osteonectin-null and haploinsufficient mice display primarily defects in trabecular bone volume.[10] Overall, these data suggest that human osteonectin 3' UTR haplotypes A and B differentially affect the trabecular bone compartment, and that $ON^{B/B}$ gained more trabecular bone with age than $ON^{A/A}$ mice.

SNP 1599 modifies the bone anabolic effect of intermittent PTH

Since intermittent administration of PTH is the best bone anabolic therapy currently available, we studied the response of $ON^{A/A}$ and $ON^{B/B}$ mice to this treatment. 10-week old male mice were injected daily with 40 μg/kg PTH (1-34) or vehicle, 5 days per week, for 4 weeks. μCT analysis showed that after 4 weeks of treatment, PTH significantly increased cortical bone area in both $ON^{A/A}$ and $ON^{B/B}$ mice, however the gain in cortical bone in $ON^{B/B}$ mice was nearly twice than that observed in $ON^{A/A}$ mice (Figure 4A, Table 3). The PTH mediated increase in the total cross-sectional area (Tt.Ar.) was greater in $ON^{B/B}$ mice compared with $ON^{A/A}$ mice, providing a mechanism for increased cortical bone area. PTH-mediated changes in marrow area (Ma.Ar.) did not reach significance ($p=0.07$) in either genotype (Figure 4A and Table 3). These data indicate that the bone anabolic effect of intermittent PTH was greater in $ON^{B/B}$ mice compared to $ON^{A/A}$.

We also assessed changes in the trabecular bone at the femoral metaphysis of PTH or vehicle injected mice using microCT. Although the PTH-mediated increase in trabecular bone volume was not statistically significant, PTH did increase trabecular thickness and number to a similar extent in mice of both genotypes (Figure 4B, Table 3). Histomorphometry was used to evaluate bone remodeling parameters and bone formation rate in femoral trabecular region of vehicle and PTH injected $ON^{A/A}$ and $ON^{B/B}$ mice.[12] Interestingly, osteoblast number was lower in vehicle treated $ON^{B/B}$ mice compared to $ON^{A/A}$, whereas bone formation rate (BFR) was higher in the vehicle treated $ON^{B/B}$ mice (Figure 4C,and D; Table 4, Figure S4). These data suggest greater bone forming activity, per cell, in $ON^{B/B}$ mice. With PTH treatment, osteoblast number and bone formation rate in both $ON^{A/A}$ and $ON^{B/B}$ mice were significantly increased, such that they were equivalent. Differences in osteoclast number and eroded surface were not seen between $ON^{A/A}$ and $ON^{B/B}$ mice, in the presence or absence of PTH treatment (Table 4). Altogether, these data indicate that $ON^{A/A}$ mice have decreased bone formation compared with $ON^{B/B}$ mice, providing an explanation for the failure of $ON^{A/A}$ mice to increase trabecular bone volume from 10 to 20 weeks of age (Figure 4D).

To determine whether PTH might have a direct effect on miR-433 expression, wild type mouse BMSCs were cultured to confluence, serum-deprived, and treated with PTH or vehicle for 3, 6, 12 or 24 hours of treatment (Figure S6). However, PTH treatment did not regulate miR-433 levels at any time point tested, suggesting that the actions of PTH on bone in vivo may not be related to direct effects on miR-433.

Cell autonomous effect of SNP 1599 on osteoblastic differentiation and mineralized matrix deposition

To determine whether the effect of SNP 1599 on bone formation was cell autonomous, we monitored osteoblastic differentiation markers in BMSCs from $ON^{A/A}$ and $ON^{B/B}$ mice cultured for up to 2 weeks. After 1 week of culture in osteoblast differentiation medium, $ON^{B/B}$ cells displayed significantly more osteocalcin and bone sialoprotein mRNA compared to $ON^{A/A}$ cultures (Figure 4E and F). After 2 weeks of culture, bone sialoprotein mRNA levels were no longer significantly different between genotypes, whereas osteocalcin mRNA remained elevated in $ON^{B/B}$ cultures.

We also assessed mineralized matrix deposition in BMSCs undergoing osteoblastic differentiation in vitro. Mineralized matrix deposition was quantified using alizarin red staining, whereas differences in cell density were monitored by crystal violet staining (Figure S5). The stains were then solubilized and quantified; and alizarin red staining was normalized to crystal violet (Figure 4G-I). Although both cultures were plated at the same density, crystal violet staining was significantly greater in $ON^{A/A}$ compared to $ON^{B/B}$ cultures (Figure 4H). Crystal violet staining peaked at week 2 in $ON^{A/A}$ cultures, and at week 3 in $ON^{B/B}$ cultures. However, despite the lower cell number, $ON^{B/B}$ cultures showed a greater alizarin red staining at weeks 3 and 4 of differentiation (Figure 4G). After normalizing alizarin red staining by crystal violet, the difference in mineralized matrix deposition between $ON^{A/A}$ and $ON^{B/B}$ cultures became more apparent (Figure 4I). This

suggests that $ON^{B/B}$ osteoblasts deposited significantly more mineralized matrix per cell compared to $ON^{A/A}$ cultures, and support the in vivo observations (Figure 4C and D).

To determine whether there were inherent differences in the growth rate of $ON^{A/A}$ and $ON^{B/B}$ BMSCs, MTS assay was used to monitor the growth of sub-confluent cultures. We found that the growth rate for $ON^{A/A}$ and $ON^{B/B}$ stromal cells did not differ (Figure S5A). Similarly, previous in vitro studies showed that osteonectin-null osteoblasts displayed decreased osteoblast maturation and mineralized matrix deposition, but no defects in cell growth.[11] The present in vitro studies support the concept that, in BMSCs, osteonectin levels do not impact cell growth, but have effects on osteoblastic differentiation.

Discussion

Skeletal phenotype is a complex genomic trait, and only a minute fraction of the genetic variants contributing to this phenotype have been identified. Further, the in vivo function of most osteoporosis-associated polymorphisms identified through GWAS and candidate gene studies is not known.[1] In this study, we developed a novel knock-in mouse model to determine the in vivo impact of a human regulatory region polymorphism on skeletal phenotype. This model demonstrated that a SNP in the osteonectin 3' UTR can regulate osteonectin levels and bone volume, essentially validating the association between osteonectin 3' UTR SNP haplotypes and bone mass first identified in a cohort of Caucasian men with idiopathic osteoporosis.[13] Moreover, we identified a potential molecular mechanism by which this SNP regulates osteonectin expression, through differential targeting of a miRNA.

Bone matrix is enriched in osteonectin. This integrin-binding matricellular protein is important for regulating collagen matrix assembly and organization.[26-28] In fact, many connective tissue pathologies detected in osteonectin-null mice have been attributed to defective extracellular matrix composition.[27-29] In vitro and in vivo studies demonstrate that collagen fibril organization is impaired in bone matrices of osteonectin-null mice, likely contributing to decreased bone mineralization.[27] In vitro, osteonectin promotes osteoblast survival, differentiation and matrix mineralization.[11] It is possible that extracellular matrix organization differs between $ON^{A/A}$ and $ON^{B/B}$ mice, which may contribute to differences in osteoblastic differentiation and mineralization; studies to address these questions are ongoing.

Although we did not analyze osteonectin mRNA or protein levels in $ON^{A/A}$ and $ON^{B/B}$ mice after PTH administration, studies by Turner et al. (2007) showed that intermittent PTH administration increased osteonectin mRNA in bone of rats subjected to hind limb unloading.[30] Previously, we reported that although osteonectin-null and haploinsufficient mice gain bone in response to intermittent PTH therapy, their bone-anabolic response was less than that seen in wild type mice. For the most part, the response of these mice to PTH could be related to osteonectin gene dosage.[12] Although the dose of PTH used in our previous study was higher than the one used in this report (80 vs 40 μg/kg/day), our results suggest that higher levels of osteonectin in bone are associated with greater PTH-mediated bone gain, particularly with regard to the cortical compartment (Figure 4A). It is possible

that the higher levels of osteonectin in $ON^{B/B}$ mice could facilitate the anabolic response of bone to intermittent PTH treatment.

The expression of osteonectin is tightly regulated through mechanisms that alter transcription, mRNA stability, and translation.[20, 23, 31-36] In osteoblasts, the osteonectin transcript is quite stable, with a half-life of >24 hours under conditions of transcription arrest.[31] Therefore, regulation of translation would likely provide the most rapid means of decreasing osteonectin synthesis. Recently, 2 evolutionarily conserved binding sites for the miR-29 family of miRNAs were found in the proximal region of the osteonectin 3' UTR.[23] Induction of miR-29 expression by canonical Wnt signaling provided potent repression of osteonectin protein synthesis, within one hour of treatment.[20] This example illustrates the efficiency by which miRNAs could regulate osteonectin levels.

In this study, we identified miR-433 as a miRNA that could play a role in regulating osteonectin expression. The mature miR-433 sequence is identical between mice and humans, and the organization of the miR-433 genomic locus conserved. Previously, miR-433 was shown to decrease during BMP2-induced osteoblastic differentiation of C3H10T1/2 cells, and to target the *Runx2* 3' UTR.[22] Our study confirms that miR-433 expression decreases during osteoblastic differentiation in human cells, and that miR-433 has an inhibitory effect on differentiation (Figure 2). We also demonstrated that SNP 1599 modulates the ability of miR-433 to regulate the human osteonectin 3' UTR (Figure 2). Although the effect of the miR-433 inhibitor on the haplotype A construct was modest, it is consistent with effects reported in other studies, and may reflect the relatively low level of miR-433 expression in the human osteoblast cell line.[18] Moreover, osteonectin is expressed in multiple tissues, many of which likely have a complement of miRNAs that are distinct from that found in the bone cells. Other miRNAs might bind to the osteonectin 3' UTR, and differential binding of these miRNAs to the region containing SNP 1599 must be strongly considered.

Others have examined the potential association of osteonectin SNPs with disease phenotype in systemic sclerosis, hepatocellular carcinoma, glaucoma, and keratoconus.[29, 37-40] Although some studies have associated particular osteonectin 3' UTR SNPs and disease, these reports have not involved SNP 1599, nor have they described potential mechanisms. Osteonectin SNP 1599G is a common variant (Table 5).[41] In a sample population of North Americans that are of African descent, frequency of the SNP1599G allele, present in haplotype A, is less than that for populations of European or Chinese descent (dbSNP summary for ss24686914). Studies have shown that, as a group, African Americans have higher bone mineral density compared to Caucasians.[42, 43] Although several candidate genes have been associated with BMD within these groups, it is not clear whether decreased frequency of SNP 1599G could play a part in this effect.[44]

In the literature, there has been argument about whether the majority of phenotypic variance is driven by rare variants with large effects or by common variants with small effects.[45] Most likely, rare and common variants work together, in conjunction with gene-environment interactions, to specify phenotype. The present study was performed in an inbred mouse strain, and the animals were housed in well-controlled environmental conditions. These

experimental parameters allowed us to decrease the impact of genetic variance and gene-environment interactions on trabecular and cortical bone phenotype. This permitted us to assign a physiological function to a common osteonectin allele, providing support for its contribution to the complex trait of skeletal phenotype.

Presently, estimation of a patient's risk of fracture is performed using models based on clinical, demographic and anthropomorphic information, such as BMD, previous fracture, a parent with hip fracture, smoking, glucocorticoid and alcohol use. Although valuable, the prognostic performance of these models could be improved especially in case of idiopathic osteoporosis. Including genetic profiling data for an individual could help improve accuracy of risk assessment and better inform treatment decisions.[46] Osteonectin SNP 1599 could be of importance to consider in investigations of idiopathic osteoporosis. However, the impact of a single variant on fracture risk is small, and identification of many more gene variants with an impact on the skeleton is necessary before real gains in fracture prediction can be realized.[46, 47] Data such as those reported here will contribute to the pool of SNP variants needed for individualized risk assessment and fracture prevention.

Supplementary Material

Refer to Web version on PubMed Central for supplementary material.

Acknowledgements

We thank Dr. Larry Fisher (NIDCR, NIH) for the gift of the BON-1 antibody, Dr. Andrea Alford (Univ. Michigan, Ann Arbor) for advice on osteonectin protein extraction, Dr. Peter Maye for BSP primers and Dr. Remegius Jackson for contributing to Luciferase reporter construction. Research reported in this publication was supported by the National Institute of Arthritis and Musculoskeletal and Skin Diseases of the National Institutes of Health under Award Number AR044877 (to AMD) and by the Center for Molecular Medicine at UConn Health. The content is solely the responsibility of the authors and does not necessarily represent the official views of the National Institutes of Health.

References

1. Stewart TL, Ralston SH. Role of genetic factors in the pathogenesis of osteoporosis. J Endocrinol. 2000; 166(2):235–45. [PubMed: 10927613]
2. Peacock M, Turner CH, Econs MJ, Foroud T. Genetics of osteoporosis. Endocr Rev. 2002; 23(3): 303–26. [PubMed: 12050122]
3. Kurt O, Yilmaz-Aydogan H, Uyar M, Isbir T, Seyhan MF, Can A. Evaluation of ERalpha and VDR gene polymorphisms in relation to bone mineral density in Turkish postmenopausal women. Mol Biol Rep. 2012; 39:6723–30. [PubMed: 22311020]
4. Yamada Y. Association of polymorphisms of the transforming growth factor-beta1 gene with genetic susceptibility to osteoporosis. Pharmacogenetics. 2001; 11:765–71. [PubMed: 11740340]
5. Shen L, Qiu Y, Xing S, et al. Association between osteoprotegerin genetic variants and bone mineral density in Chinese women. Int Immunopharmacol. 2013; 16(2):275–8. [PubMed: 23619553]
6. Falcon-Ramirez E, Casas-Avila L, Miranda A, Diez P, Castro C, Rubio J, et al. Sp1 polymorphism in collagen I alpha1 gene is associated with osteoporosis in lumbar spine of Mexican women. Mol Biol Rep. 2011; 38:2987–92. [PubMed: 20146006]
7. Koller DL, Econs MJ, Morin PA, et al. Genome screen for QTLs contributing to normal variation in bone mineral density and osteoporosis. J Clin Endocrinol Metab. 2000; 85(9):3116–20. [PubMed: 10999795]

8. Kapinas K, Kessler CB, Delany AM. miR-29 suppression of osteonectin in osteoblasts: regulation during differentiation and by canonical Wnt signaling. J Cell Biochem. 2009; 108(1):216–24. [PubMed: 19565563]
9. Boskey AL, Moore DJ, Amling M, Canalis E, Delany AM. Infrared analysis of the mineral and matrix in bones of osteonectin-null mice and their wildtype controls. J Bone Miner Res. 2003; 18(6):1005–11. [PubMed: 12817752]
10. Delany AM, Amling M, Priemel M, Howe C, Baron R, Canalis E. Osteopenia and decreased bone formation in osteonectin-deficient mice. J Clin Invest. 2000; 105(9):1325. [PubMed: 10792008]
11. Delany AM, Kalajzic I, Bradshaw AD, Sage EH, Canalis E. Osteonectin-null mutation compromises osteoblast formation, maturation, and survival. Endocrinology. 2003; 144(6):2588–96. [PubMed: 12746322]
12. Machado do Reis L, Kessler CB, Adams DJ, Lorenzo J, Jorgetti V, Delany AM. Accentuated osteoclastic response to parathyroid hormone undermines bone mass acquisition in osteonectin-null mice. Bone. 2008; 43(2):264–73. [PubMed: 18499553]
13. Delany AM, McMahon DJ, Powell JS, Greenberg DA, Kurland ES. Osteonectin/SPARC polymorphisms in Caucasian men with idiopathic osteoporosis. Osteoporos Int. 2008; 19(7):969–78. [PubMed: 18084690]
14. Kurland ES, Rosen CJ, Cosman F, McMahon D, Chan F, et al. Insulin-like growth factor-I in men with idiopathic osteoporosis. J Clin Endocrinol Metab. 1997; 82:2799–2805. [PubMed: 9284699]
15. Kurland ES, Chan FK, Rosen CJ, Bilezikian JP. Normal growth hormone secretory reserve in men with idiopathic osteoporosis and reduced circulating levels of insulin-like growth factor-I. J Clin Endocrinol Metab. 1998; 83:2576–2579. [PubMed: 9661647]
16. Mendell JT, Dietz HC. When the message goes awry: disease-producing mutations that influence mRNA content and performance. Cell. 2001; 107(4):411–4. Review. [PubMed: 11719181]
17. Lei SF, Papasian CJ, Deng HW. Polymorphisms in predicted miRNA binding sites and osteoporosis. J Bone Miner Res. 2011; 26(1):72–8. [PubMed: 20641033]
18. Simon D, Laloo B, Barillot M, et al. A mutation in the 3'-UTR of the HDAC6 gene abolishing the post-transcriptional regulation mediated by hsa-miR-433 is linked to a new form of dominant X-linked chondrodysplasia. Hum Mol Genet. 2010; 19(10):2015–27. [PubMed: 20181727]
19. Harris SA, Enger RJ, Riggs BL, Spelsberg TC. Development and characterization of a conditionally immortalized human fetal osteoblastic cell line. J Bone Miner Res. 1995; 10(2):178–86. [PubMed: 7754797]
20. Kapinas K, Kessler C, Ricks T, Gronowicz G, Delany AM. miR-29 modulates Wnt signaling in human osteoblasts through a positive feedback loop. J Biol Chem. 2010; 285(33):25221–31. [PubMed: 20551325]
21. Rehmsmeier M, Steffen P, Hochsmann M, Giegerich R. Fast and effective prediction of microRNA/target duplexes. RNA. 2004; 10(10):1507–17. [PubMed: 15383676]
22. Kim EJ, Kang IH, Lee JW, Jang WG, Koh JT. MiR-433 mediates ERRγ-suppressed osteoblast differentiation via direct targeting to Runx2 mRNA in C3H10T1/2 cells. Life Sci. 2013; 92(10): 562–8. [PubMed: 23353875]
23. Kapinas K, Kessler CB, Delany AM. miR-29 suppression of osteonectin in osteoblasts: regulation during differentiation and by canonical Wnt signaling. J Cell Biochem. 2009; 108(1):216–24. [PubMed: 19565563]
24. Sheng MH, Lau KH, Beamer WG, Baylink DJ, Wergedal JE. In vivo and in vitro evidence that the high osteoblastic activity in C3H/HeJ mice compared to C57BL/6J mice is intrinsic to bone cells. Bone. 2004; 35:711–719. [PubMed: 15336608]
25. Shultz KL, Donahue LR, Bouxsein ML, Baylink DJ, Rosen CJ, Beamer WG. Congenic strains of mice for verification and genetic decomposition of quantitative trait loci for femoral bone mineral density. J Bone Miner Res. 2003; 18:175–185. [PubMed: 12568393]
26. Bradshaw AD, Sage EH. SPARC, a matricellular protein that functions in cellular differentiation and tissue response to injury. J Clin Invest. 2001; 107(9):1049–54. [PubMed: 11342565]
27. Kapinas K, Lowther KM, Kessler CB, et al. Bone matrix osteonectin limits prostate cancer cell growth and survival. Matrix Biol. 2012; 31(5):299–307. [PubMed: 22525512]

28. Rentz TJ, Poobalarahi F, Bornstein P, Sage EH, Bradshaw AD. SPARC regulates processing of procollagen I and collagen fibrillogenesis in dermal fibroblasts. J Biol Chem. 2007; 282:22062–22071. [PubMed: 17522057]
29. Chen LJ, Tam PO, Tham CC, et al. Evaluation of SPARC as a candidate gene of juvenile-onset primary open-angle glaucoma by mutation and copy number analyses. Mol Vis. 2010; 16:2016–2025. [PubMed: 21042566]
30. Turner RT, Evan GL, Lotinun S, Lapke PD, Iwaniec UT, et al. Dose-Response effects of intermittent PTH on cancellous bone in hindlimb unloaded rats. J Bone Miner Res. 2007; 22:64–71. [PubMed: 17042715]
31. Delany AM, Canalis E. Basic fibroblast growth factor destabilizes osteonectin mRNA in osteoblasts. Am J Physiol. 1998; 274(3 Pt. 1):734–40.
32. Chamboredon S, Briggs J, Vial E, et al. v-Jun downregulates the SPARC target gene by binding to the proximal promoter indirectly through Sp1/3. Oncogene. 2003; 22:4047–4061. [PubMed: 12821939]
33. Dominguez P, et al. Expression of the osteonectin gene potentially controlled by multiple cis- and trans-acting factors in cultured bone cells. J Bone Miner Res. 1991; 6:1127–1136. [PubMed: 1796760]
34. Ibaraki K, Robey PG, Young MF. Partial characterization of a novel 'GGA' factor which binds to the osteonectin promoter in bovine bone cells. Gene. 1993; 130:225–232. [PubMed: 8359689]
35. Ng KW, Manji SS, Young MF, Findlay DM. Opposing influences of glucocorticoid and retinoic acid on transcriptional control in preosteoblasts. Mol Endocrinol. 1989; 3:2079–2085. [PubMed: 2628742]
36. Sauk JJ, Norris K, Kerr JM, Somerman MJ, Young MF. Diverse forms of stress result in changes in cellular levels of osteonectin/SPARC without altering mRNA levels in osteoligament cells. Calcif Tissue Int. 1991; 49:58–62. [PubMed: 1893297]
37. De Bonis P, Laborante A, Pizzicoli C, et al. Mutational screening of VSX1, SPARC, SOD1, LOX, and TIMP3 in keratoconus. Mol Vis. 2011; 17:2482–2494. [PubMed: 21976959]
38. Lagan AL, Pantelidis P, Renzoni EA, et al. Single-nucleotide polymorphisms in the SPARC gene are not associated with susceptibility to scleroderma. Rheumatology. 2005; 44:197–201. [PubMed: 15546965]
39. Segat L, Milanese M, Pirulli D, et al. Secreted protein acidic and rich in cysteine (SPARC) gene polymorphism association with hepatocellular carcinoma in Italian patients. J Gastroenterol Hepatol. 2009; 24:1840–1846. [PubMed: 19817957]
40. Zhou X, Tan FK, Reveille JD, et al. Association of novel polymorphisms with the expression of SPARC in normal fibroblasts and with susceptibility to scleroderma. Arthritis Rheum. 2002; 46:2990–2999. [PubMed: 12428242]
41. Sherry ST, Ward MH, Kholodov M, Baker J, Phan L, Smigielski EM, Sirotkin K. dbSNP: the NCBI database of genetic variation. Nucleic Acids Res. 2001; 29:308–311. [PubMed: 11125122]
42. Hochberg MC. Racial differences in bone strength. Trans Am Clin Climatol Assoc. 2007; 118:305–15. [PubMed: 18528512]
43. George A, Tracy JK, Meyer WA, Flores RH, Wilson PD, Hochberg MC. Racial differences in bone mineral density in older men. J Bone Miner Res. 2003; 18:2238–44. [PubMed: 14672360]
44. Gong G, Haynatzki G, Haynatzka V, Howell R, Kosoko-Lasaki S, Fu YX, Yu F, Gallagher JC, Wilson MR. Bone mineral density-affecting genes in Africans. J Natl Med Assoc. 2006; 98(7): 1102–8. [PubMed: 16895279]
45. Gibson G. Rare and common variants: twenty arguments. Nat Rev Genet. 2012; 13:135–145. [PubMed: 22251874]
46. Nguyen TV, Eisman JA. Genetics and the individualized prediction of fracture. Curr Osteoporos Rep. 2012; 10:236–244. [PubMed: 22851044]
47. Mitchell BD, Streeten EA. Clinical impact of recent genetic discoveries in osteoporosis. Appl Clin Genet. 2013; 6:75–85. [PubMed: 24133373]

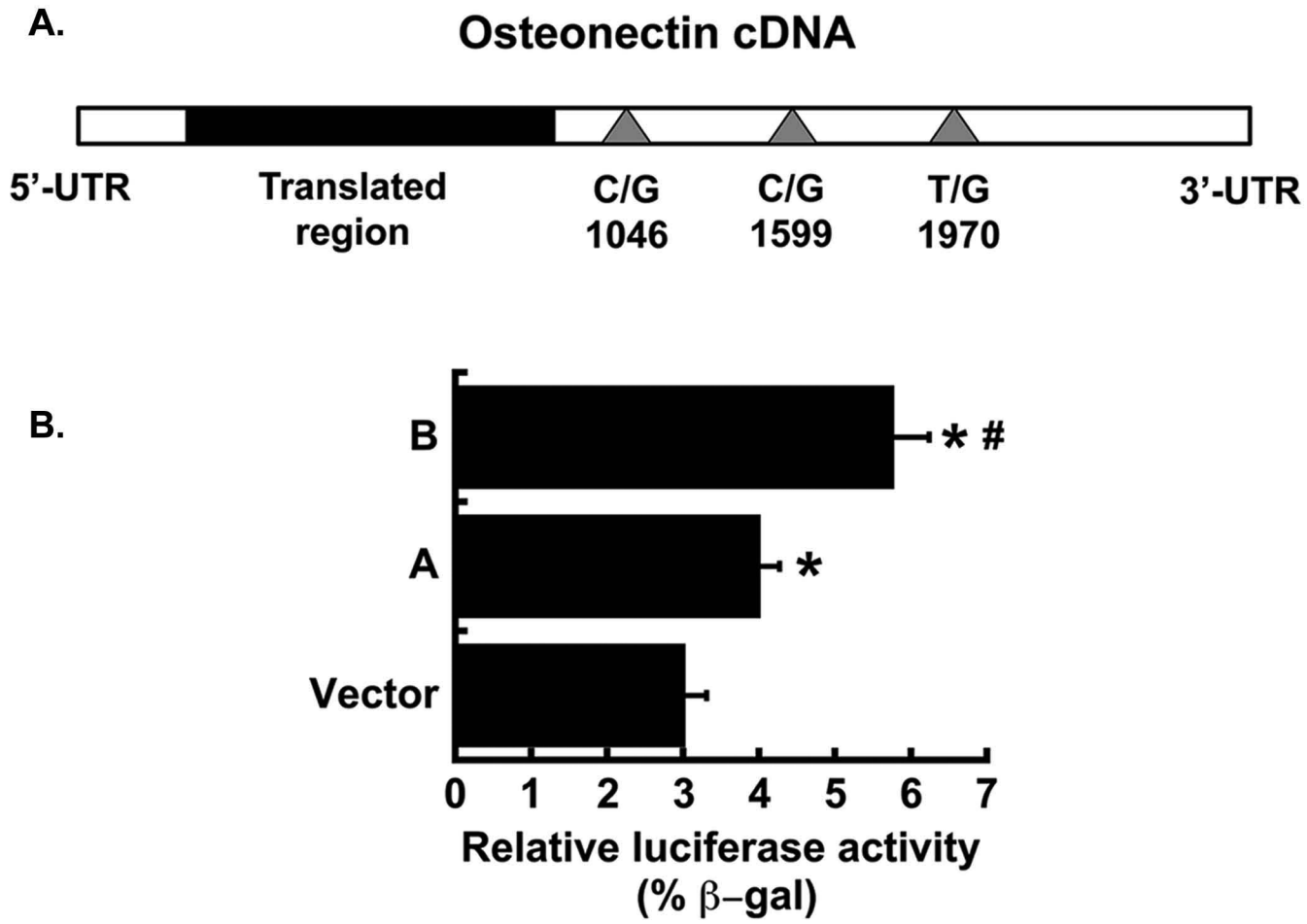

Figure 1. Osteonectin 3' UTR SNP 1599 regulates 3' UTR function

(*A*) Schematic representation of the human osteonectin cDNA, and the characterized SNPs at bases 1046, 1599 and 1970 (grey triangles). (*B*) Human ON 3' UTR (cDNA bases 1018-2123) representing haplotypes A and B were cloned into pMIR-REPORT Luciferase vector. Luciferase activity was quantified in hFOB1.19 cells and normalized to β-galactosidase activity (*$p<0.05$ different from vector; # $p<0.05$ different from haplotype A, N=6).

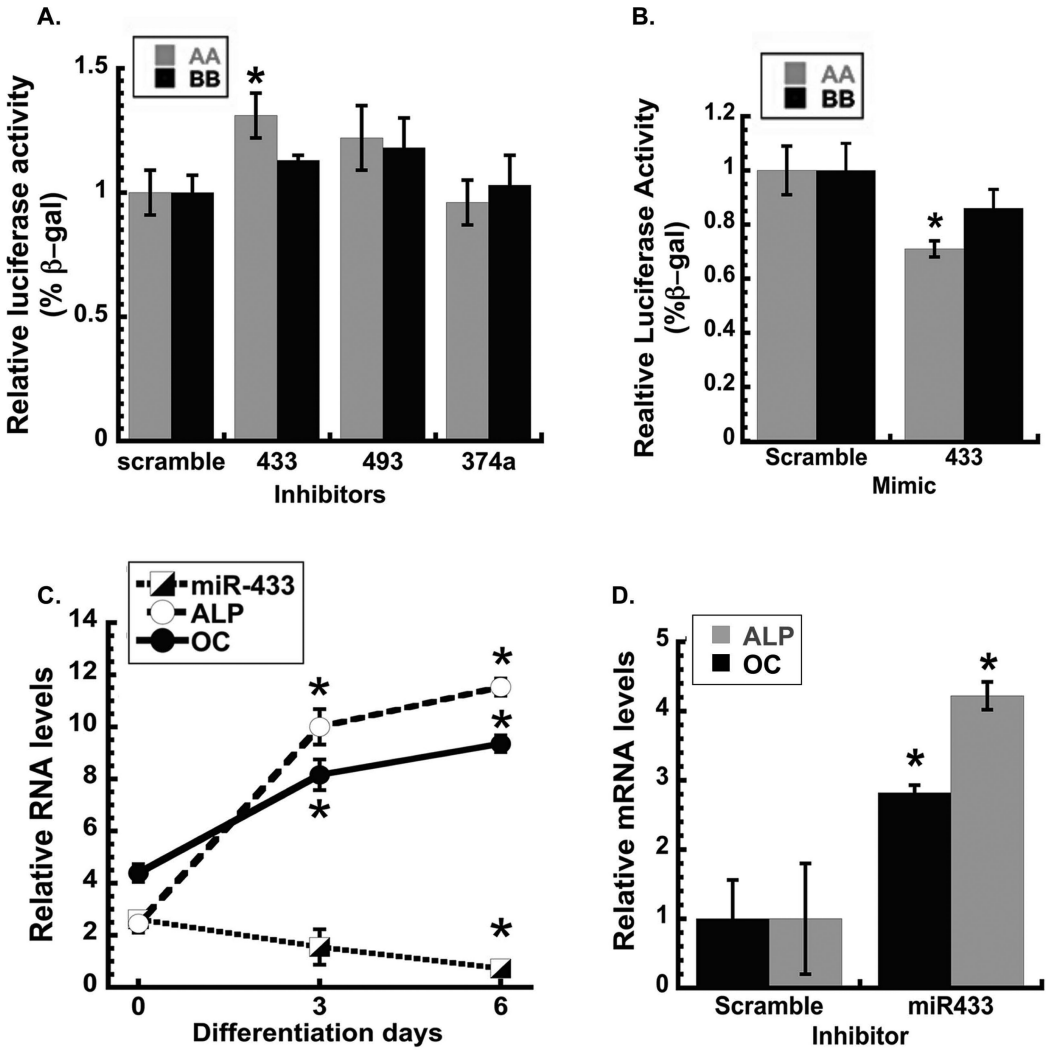

Figure 2. miR-433 represses haplotype A 3' UTR and decreases during osteoblastic differentiation in vitro

Luciferase activity of haplotype A and B pMIR-report constructs in hFOB1.19 cells co-transfected with specific miRNA inhibitors or scramble control. Inhibitors for miR-433, -493 and -374a (*A*) and miR-433 mimic or scramble control mimic *(B)* were tested; luciferase activity was normalized to β-galactosidase activity (* $p<0.05$ different from scramble control, N=6). (*C*) miR-433, alkaline phosphatase (ALP) and osteocalcin (OC) RNA in hFOB 1.19 cells at confluence (0), and during osteoblastic differentiation. miR-433 normalized to RNU48; ALP and OC mRNA normalized to 18s RNA (*$p<0.05$ different from confluence, N=3). (*D*) ALP and OC RNA in hFOB1.19 cells transfected with miR-433 or scramble inhibitor and cultured in osteoblast differentiation medium for 3 days (*$p<0.05$ different from scramble inhibitor, N=3).

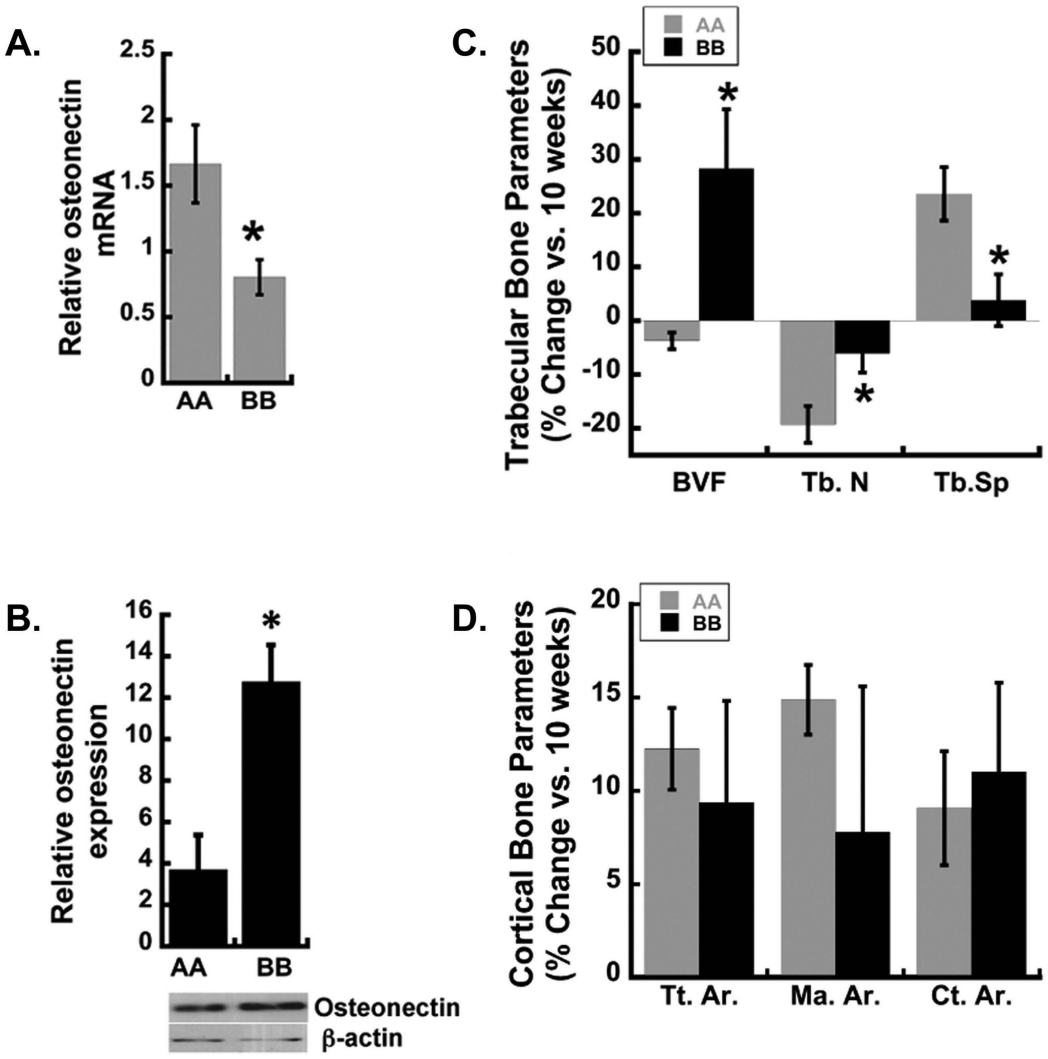

Figure 3. Osteonectin levels and gain in trabecular bone is higher in haplotype B knock-in mice

(*A*) Osteonectin mRNA was quantified by qRT-PCR using RNA isolated from the femurs of 6-8 week old $ON^{A/A}$ and $ON^{B/B}$ mice. Osteonectin mRNA levels were normalized to 18s RNA (N=4 mice/ haplotype, * $p<0.05$ different from haplotype A). *(B)* Western blotting for osteonectin and β-actin in lysates from long bones of $ON^{A/A}$ and $ON^{B/B}$ mice (*$p<0.05$ different from haplotype A, N=3 mice/group). (*C*, *D*) μCT analysis of changes in femoral bone from 10 to 20 weeks of age in $ON^{A/A}$ and $ON^{B/B}$ mice. Trabecular bone volume (BVF), trabecular bone number (Tb.N) trabecular bone spacing (Tb.Sp.). Total (periosteal) area (Tt.Ar), marrow area (Ma.Ar), cortical area (Ct.Ar). *$p<0.05$ different from haplotype A, N=4-9 mice/group.

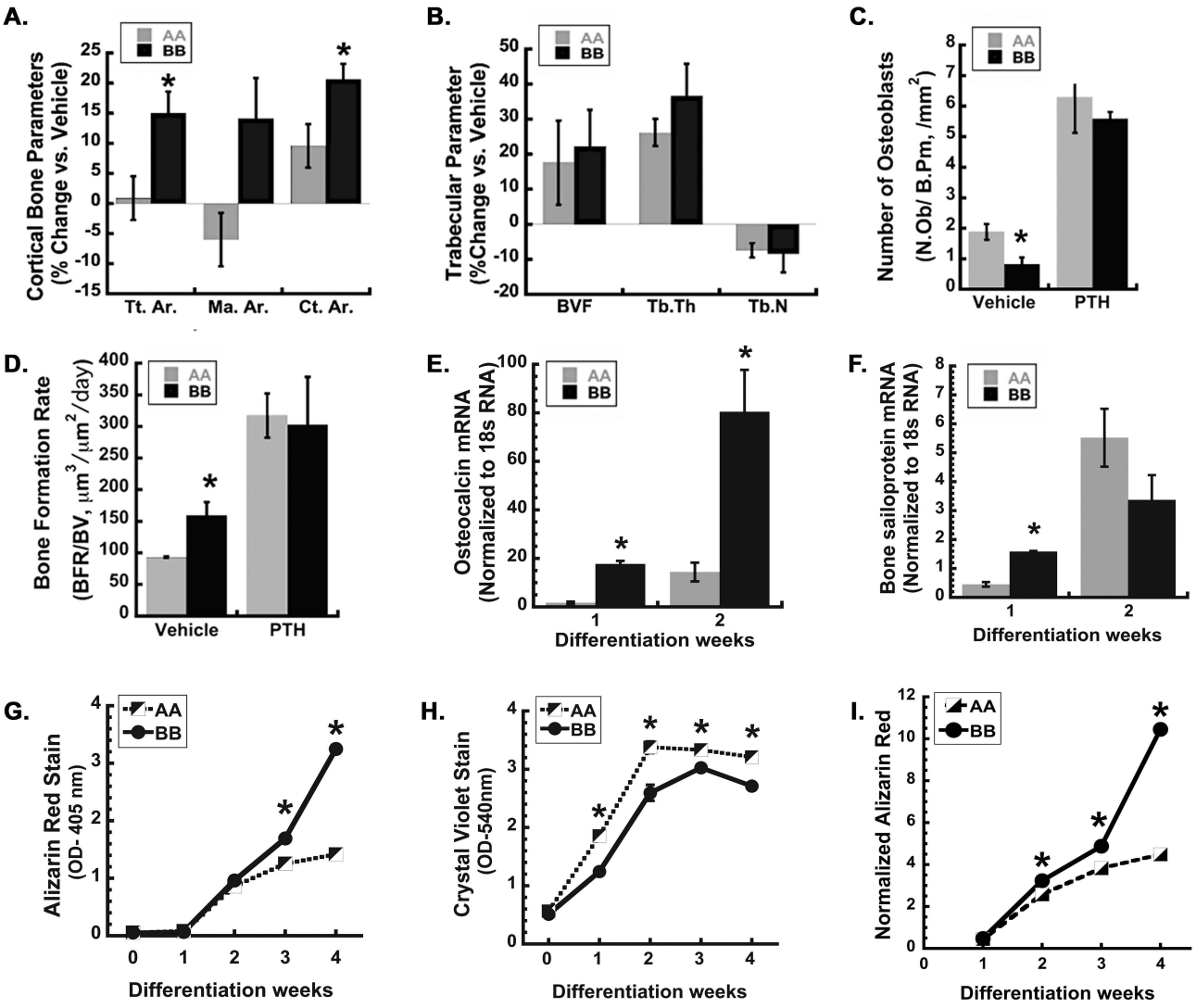

Figure 4. PTH induced gain of cortical bone area is greater in haplotype B knock-in mice, and BMSCs from haplotype B mice have enhanced osteoblastic differentiation in vitro

µCT and histomorphometric analysis of femoral trabecular bone from 14-week old $ON^{A/A}$ and $ON^{B/B}$ mice that had been injected for 4 weeks with 40 µg/kg/day PTH or vehicle. (*A*) Percent change in cortical bone parameters vs. vehicle in femur. Total (periosteal) area (Tt.Ar), marrow area (Ma.Ar), cortical area (Ct.Ar). (*B*) Percent change in trabecular bone parameters vs. vehicle in femur. Trabecular bone volume (BVF), trabecular thickness (Tb.Th), trabecular bone number (Tb.N). Histomorphometric analysis of osteoblast number and bone formation rate (*C and D*) in femoral trabecular bones of vehicle and PTH treated $ON^{A/A}$ and $ON^{B/B}$ mice (*p<0.05 different from $ON^{A/A}$ mice, N=4-6/group). Osteocalcin *(E)* and Bone sailoprotein *(F)* RNA in BMSCs from $ON^{A/A}$ and $ON^{B/B}$ mice undergoing osteoblastic differentiation for 2 weeks (*p<0.05 different from $ON^{A/A}$, N=3). Quantified alizarin red *(G)* and crystal violet *(H)* staining, and alizarin red stain normalized to crystal violet *(I)* for BMSCs from $ON^{A/A}$ and $ON^{B/B}$ mice undergoing osteoblastic differentiation for up to 4 weeks (*p<0.05 different from $ON^{A/A}$, N = 4).

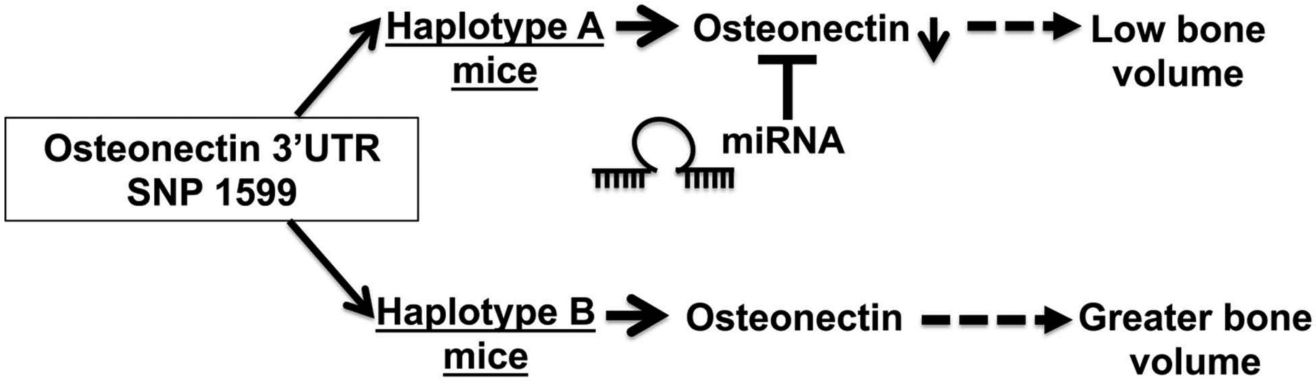

Figure 5. Working model for osteonectin 3' UTR SNP mediated effect on bone

In haplotype A knock-in mice, osteonectin levels in bone are lower compared to haplotype B knock-in mice. The osteonectin 3' UTR haplotype A is targeted by miRNA (miR-433), which may contribute to lower osteonectin and lower bone volume.

Table 1

RNAhybrid analysis of putative miR-433, -493 and -374 binding sites in osteonectin 3' UTR. SNP 1599 G/C is underlined and indicated by larger font in the seed binding region of haplotype A or B 3'. UTR.

miRNA	Haplotype A – SNP1599G	Haplotype B – SNP1599C
433-3p	target 5′A GAAAGAUUCU G A 3′ ACUGA GGGGCU UGUUAUGA UGGCU CCUCGG GUAGUACU miRNA 3′UC A 5′	target 5′A GAAAGAUUCU GUC A 3′ ACUGA GGGGCU UUAUGA UGGCU CCUCGG AGUACU miRNA 3′UC GU A 5′
493-5p	target 5′ A AUU GGG U A 3′ GAAAG CU GCUGUG UAUGA CUUUC GA UGGUAC AUGUU miRNA 3′ UUA G 5′	target 5′ C AAAG C GG U 3′ UGAGAG AUU UG GC ACUUUC UGG AC UG miRNA 3′ UU GGA U A UU 5′
374a-3p	target 5′ C G C A 3′ U GGG UGUGUUAUGA A UCC ACAUAAUAUU miRNA 3′ GUGAAU G A 5′	target 5′ C G C C A 3′ U GGG UGU UUAUGA A UCC ACA AAUAUU miRNA 3′ GUGAAU G A U 5′

Table 2

MicroCT analysis of trabecular and cortical bone parameters in femur of 10-week and 20-week old male $ON^{A/A}$ and $ON^{B/B}$ mice.

Trabecular parameters	AA		BB	
	10 weeks	20 weeks	10 weeks	20 weeks
BVF (%)	0012.60±0.010	0012.20±0.00	0011.70±0.02	0014.80±0.01*
Tb.Th.(μm)	045.48±3.72	0046.97±1.23	0053.06±2.76	0055.24±1.89*
Tb.N.(/mm)	005.20±0.33	0004.20±0.18	004.47±0.30	0004.23±0.14
Tb.Sp.(μm)	192.25±11.97	237.56±9.59	225.06±17.56	232.34±9.46

Cortical parameters	AA		BB	
	10 weeks	20 weeks	10 weeks	20 weeks
Tt.Ar.(mm^2)	1.96±0.10	2.24±0.04	1.89±0.03	2.06±0.11
Ma.Ar.(mm^2)	1.08±0.04	1.24±0.02	1.00±0.03	00001.08±0.08
Ct.Ar.(mm^2)	0.88±0.06	0.96±0.03	0.88±0.02	0.98±0.04

Trabecular bone volume fraction (BVF), trabecular bone number (Tb.N) trabecular bone spacing (Tb.Sp.) and trabecular thickness (Tb.Th.). Total (periosteal) area (Tt.Ar.), marrow area (Ma.Ar.), cortical area (Ct.Ar.). (10 weeks; N = 4-5 mice per group) (20 weeks; N = 8-9 mice per group). Mean ± SEM.

* $p<0.05$ different from haplotype A

Table 3

MicroCT analyses of trabecular and cortical bone parameters in femur of vehicle and PTH injected $ON^{A/A}$ and $ON^{B/B}$ mice.

Trabecular parameters	AA		BB	
	Vehicle	PTH	Vehicle	PTH
BVF (%)	12.00±0.01	14.00±0.01	12.00±0.01	16.00±0.01
Tb.Th.(μm)	47.03±1.16	59.54±1.94#	46.40±2.54	61.65±3.81#
Tb.N.(/mm)	4.43±0.04	4.10±0.16 #	4.72±0.16	4.25±0.21

Cortical parameters	AA		BB	
	Vehicle	PTH	Vehicle	PTH
Tt.Ar. (mm^2)	2.15±0.07	2.17±0.08	2.00±0.05	2.36±0.06 #
Ma.Ar. (mm^2)	1.22±0.06	1.15±0.05	1.10±0.03	1.21±0.07
Ct.Ar. (mm^2)	0.93±0.02	1.02±0.02 #	0.90±0.02	1.09±0.02 #

14-week old male haplotype A and B knock-in mice had been injected for 4 weeks with 40 [μg/kg/day PTH or vehicle. Trabecular bone volume fraction (BVF), trabecular bone number (Tb.N) trabecular bone spacing (Tb.Sp.) and trabecular number (Tb.N.). Total (periosteal) area (Tt.Ar.), marrow area (Ma.Ar.), cortical area (Ct. Ar.). (N=4-6 mice per group) Mean ± SEM.

# $p<0.05$ different from corresponding vehicle injected mice of the same genotype.

Table 4

Histomorphometric analysis of femoral trabecular bone of vehicle and PTH injected $ON^{A/A}$ and $ON^{B/B}$ mice.

Histomorphometry	AA		BB	
Formation	**Vehicle**	**PTH**	**Vehicle**	**PTH**
Osteoblast number (N.Ob/B.Pm, /mm^2)	1.64±0.26	6.28±1.16$^{\#}$	0.91±0.23*	6.39±1.52$^{\#}$
Mineralizing surface (MS/BS, %)	4.77±0.55	10.58±1.63$^{\#}$	7.34±0.90*	8.86±1.16
Bone formation rate (μm^3/μm^2/ day)	93.29±1.17	317.27±35.02$^{\#}$	168.36±21.90*	196.81±21.34

	AA		BB	
Resorption	**Vehicle**	**PTH**	**Vehicle**	**PTH**
Osteoclast number (N.Oc/B.Pm; /mm^2)	0.91±0.22	0.81±0.25	0.72±0.07	0.80±0.21
Osteoclast surface (Oc.S/BS, %)	2.54±0.64	2.27±0.66	1.97±0.21	2.26±0.10
Eroded surface (ES/BS, %)	5.67±1.14	5.63±1.05	4.76±0.53	5.29±0.38

14-week old haplotype A and B knock-in mice had been injected for 4 weeks with 40 μg/kg/day PTH or vehicle (N = 4-6 mice per group)

$^{\#}$p±0.05 different from the corresponding vehicle injected mice of the same genotype. Mean ± SEM.

*p<0.05 different from haplotype A mice in the same treatment group.

Table 5

Osteonectin SNP 1599 (rs1054204) allele and genotype frequencies (from dbSNP summary for ss24686914). [41]

Population ID	Ethnicity	Allele Frequency	Genotype Frequency
AFD EUR Panel-North America	European	C=0.521 G=0.479	C/G=0.542 C/C=0.208 G/G=0.250
AFD CHN Panel-North America	Asian	C=0.604 G=0.396	C/G=0.542 C/C=0.333 G/G=0.125
AFD AFR Panel-North America	African	C=0.783 G=0.217	C/G=0.348 C/C=0.609 G/G=0.043